FUNDAMENTALS OF NUCLEATION AND GROWTH OF NANOCRYSTALLINE FILMS

Liudmila A. Pozhar

Oak Ridge National Laboratory, Oak Ridge, TN
University of Tennessee, Knoxville, TN
and

Michael Z.-C. Hu

Oak Ridge National Laboratory, Oak Ridge, TN

CONTENTS

1. STATISTICAL MECHANICS: PREDICTION OF PHYSICAL PROPERTIES AND PROCESS EQUATIONS.
2. NANOCLUSTER DESIGN APPROACH: EXPERIMENTAL FINDINGS.
3. STATISTICAL MECHANICAL THEORY/EMD/NEMD: PREDICTIONS AND MODELING
4. CONCLUSIONS

MAJOR REFERENCES

1. L.A. Pozhar, *Transport Theory of Inhomogeneous Fluids* (World Scientific, New Jersey, 1994).
2. L.A. Pozhar, *Phys. Rev.* ***E*** 61, 1432 (2000).
3. L.A. Pozhar and K.E. Gubbins, *Phys. Rev.* ***E*** **56**, 5367 (1997).
4. L.A. Pozhar and K.E. Gubbins, *J. Chem. Phys.* **94**, 1367 (1991).
5. J.M.D. MacElroy, L.A. Pozhar and S.-H. Suh, Colloids and Interfaces ***A 187-188***, 493 (2001).
6. J.K. Percus, L.A. Pozhar, and K.E. Gubbins, *Phys. Rev.* ***E*** **51**, 261 (1995); L.A. Pozhar, K.E. Gubbins, and J.K. Percus, *Phys. Rev.* ***E*** **48**, 1819 (1993).

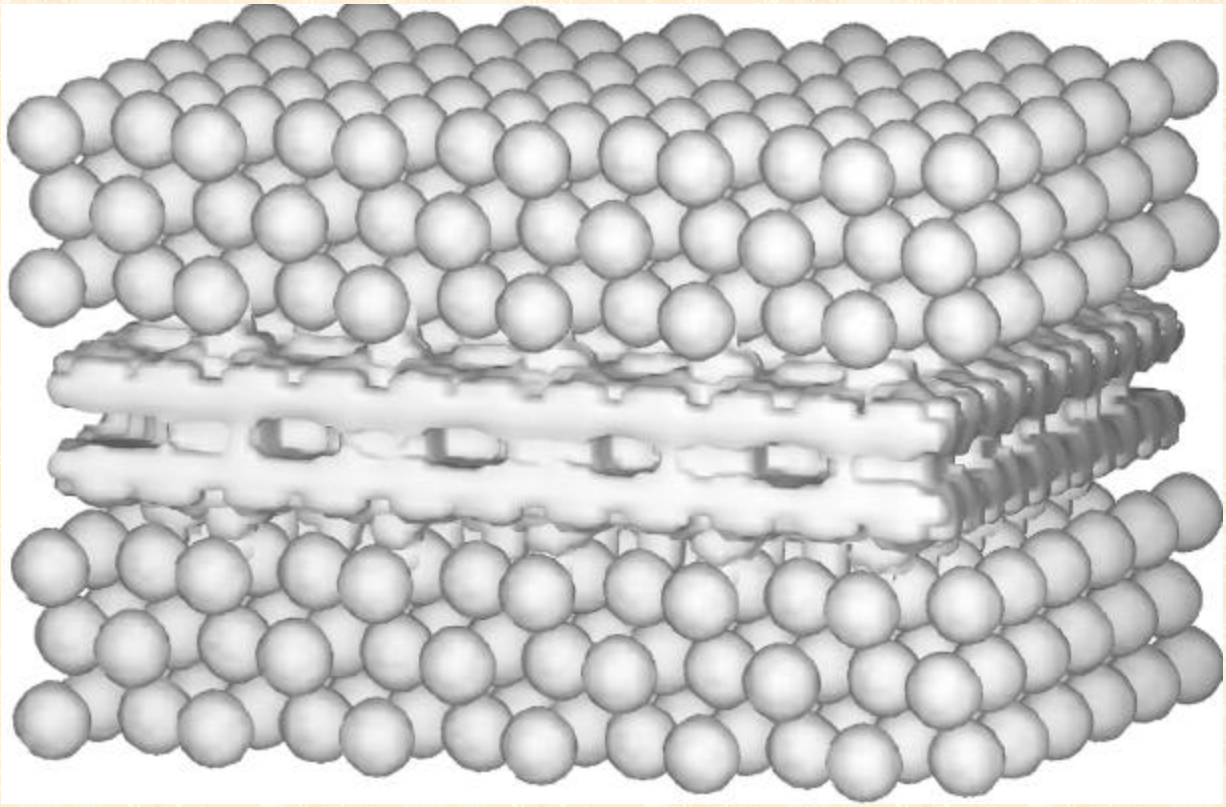

Figure 1. A model Lennard-Jones nanofluid in a slit nanopore of 3.2 s in width composed of immobile wall atoms: the 3D image of the nanofluid number density, $n s^3$, where s is the effective diameter of nanofluid atoms. The average nanofluid density $< n s^3 > = 0.603$, temperature $k_B T/e = 0.958$; k_B – the Boltzmann constant; e - the energy parameter of the Lennard-Jones potential.

1. STATISTICAL MECHANICS: PREDICTION OF PHYSICAL PROPERTIES AND PROCESS EQUATIONS

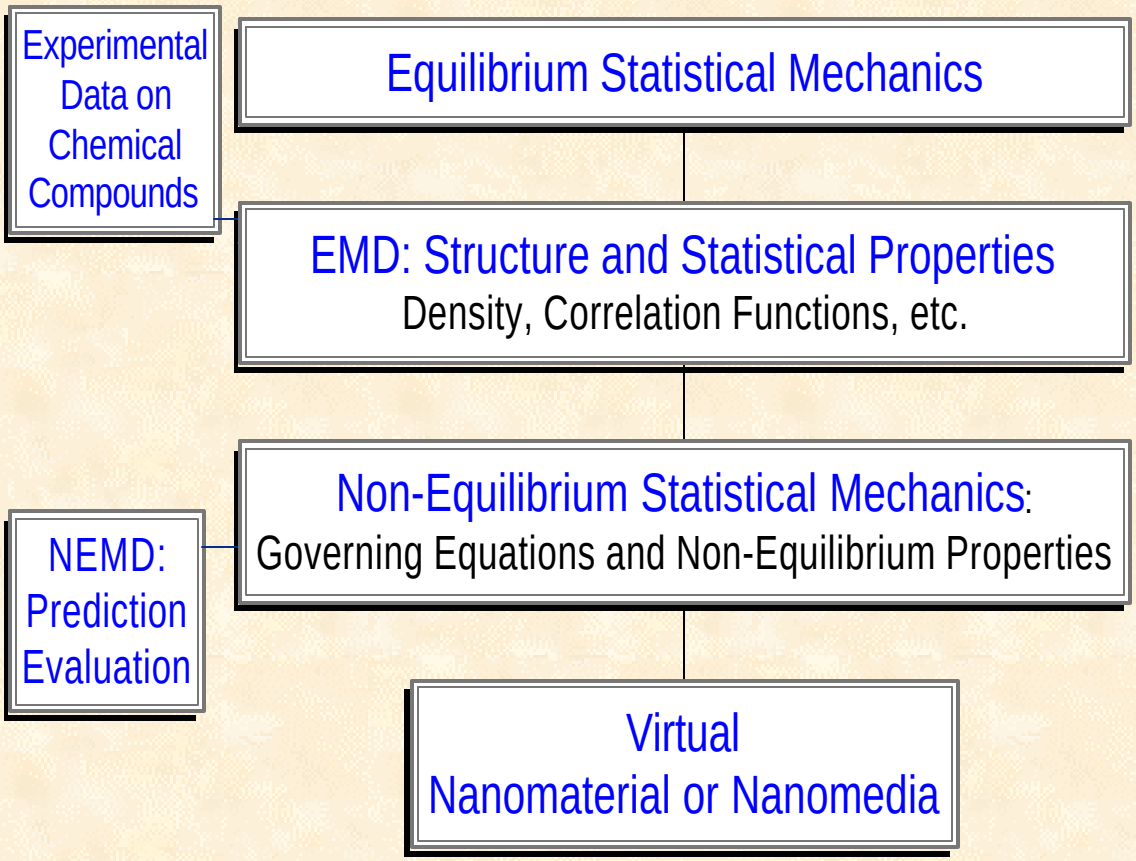

2. NANOCLUSTER DESIGN APPROACH: EXPERIMENTAL FINDINGS

Example 1. Deposition of self-assembled monolayers

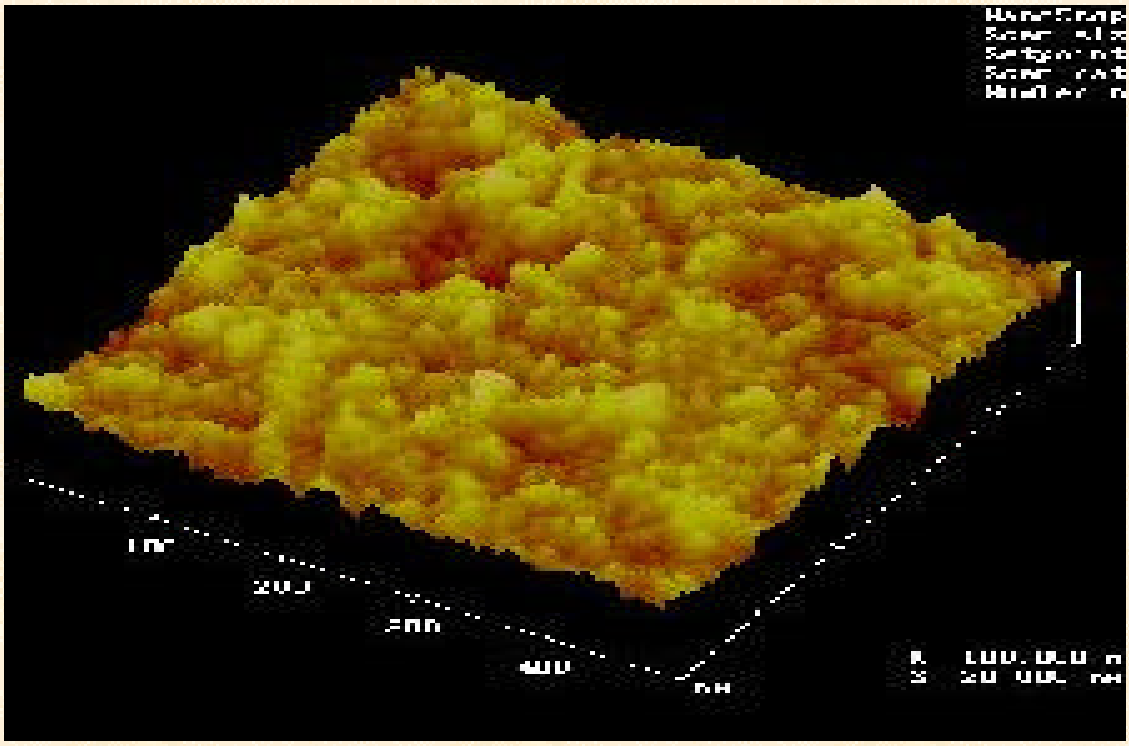

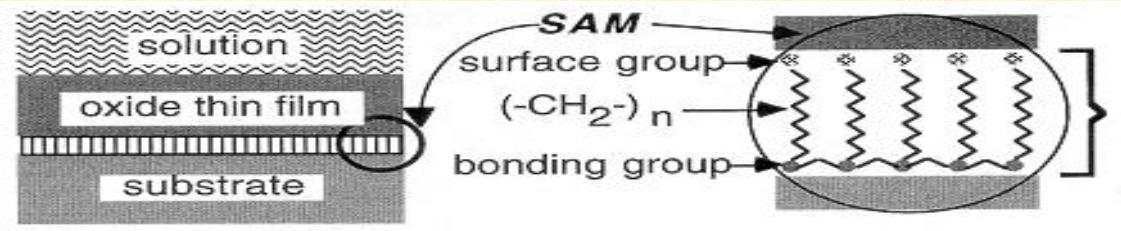

Example 2: Nanocluster design: TiO_2 films

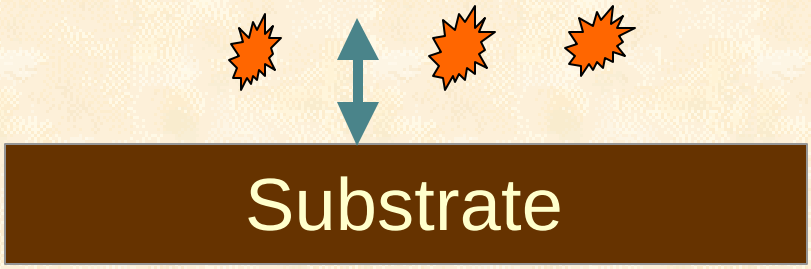

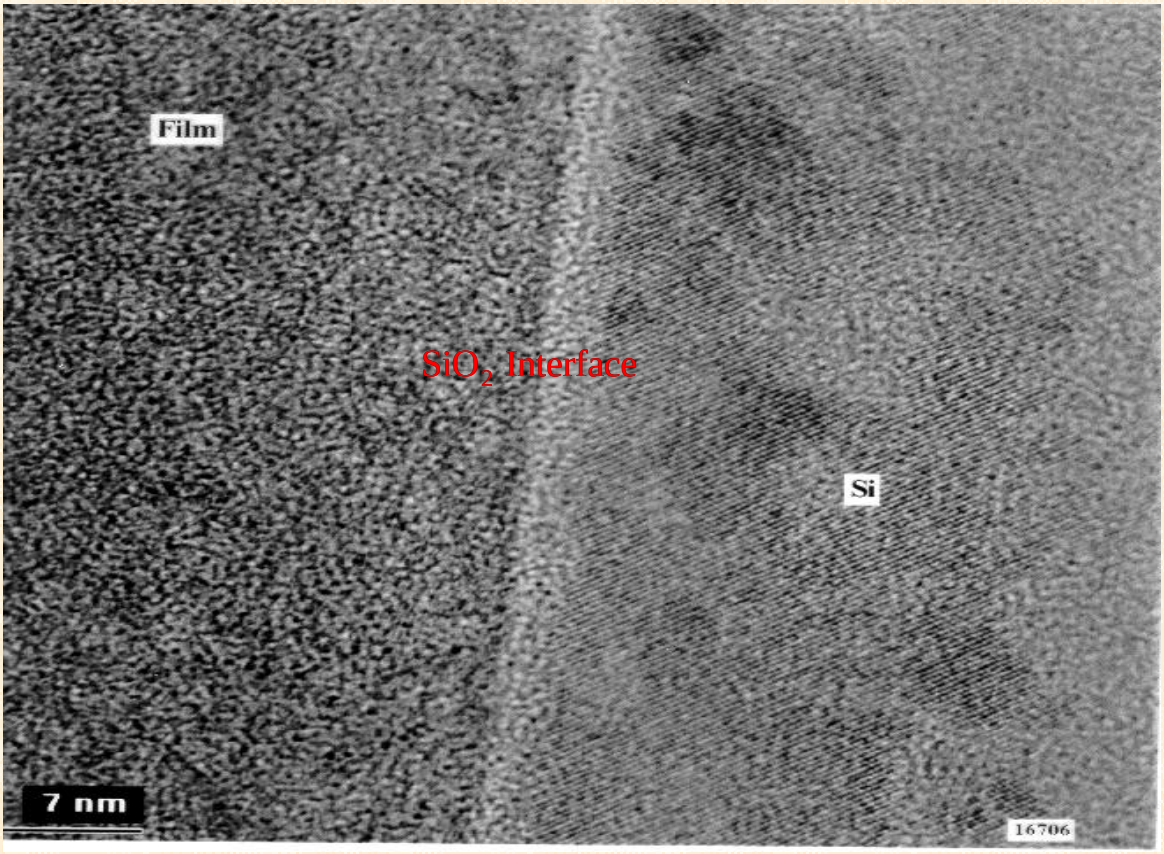

High-resolution transmission electron micrograph (cross section) of a high-quality optical titania thin film on a single-crystal silicon wafer.

3. THEORY/EMD/NEMD: PREDICTIONS AND MODELING.

A) PG-theoretical diffusion in classical nanosystems

$$\hat{\mathbf{D}}_T(\mathbf{q}) = \frac{3\tau_d(\mathbf{q})}{2\sigma^2 n_1(\mathbf{q})}\sqrt{\frac{\pi\beta}{m}}\,\hat{\mathbf{D}}(\mathbf{q}), \tag{1}$$

$$\tau_d^{-1}(\mathbf{q}) = \int d\hat{\mathbf{s}}\, n(\mathbf{q}-\sigma\hat{\mathbf{s}})\, g(\mathbf{q},\mathbf{q}-\sigma\hat{\mathbf{s}}) + \frac{\sqrt{2}\sigma_{fw}^2}{\sigma^2}\int d\hat{\mathbf{s}}\, n_w(\mathbf{q}-\sigma_{fw}\hat{\mathbf{s}})\, g_{fw}(\mathbf{q},\mathbf{q}-\sigma_{fw}\hat{\mathbf{s}})$$

$\mathbf{q}$ - a position within the fluid; σ, σ_w and σ_{fw} - the effective diameters of the hard-core contributions to the potentials of intermolecular interactions of the fluid molecules, wall molecules, and fluid and wall molecules, respectively; $\beta = 1/k_BT$, k_B is the Boltzmann constant, T is temperature, m is the mass of a fluid molecule; $n_1(\mathbf{q})$, $n(\mathbf{q})$ and $n_w(\mathbf{q})$ are the equilibrium number densities of the tracer "component" 1, the fluid "mixture" and the walls, respectively; g and g_{fw} are the contact values of the equilibrium fluid-fluid and fluid-wall pair correlation functions (PCFs), respectively, and the integrals are over the surface of the unit sphere ($\hat{\mathbf{s}}$ is the unit vector).

The Cartesian tensor $\mathbf{D}(\mathbf{q})$ in Eq. (1) has the form.

$$\hat{\mathbf{D}}(\mathbf{q}) = \frac{1}{\beta}\left[\mathbf{I}+\mathbf{F}\{n\}\right] \tag{2}$$

$\mathbf{I}$ is the unit matrix; $\mathbf{F}\{n\}$ is a functional of the fluid density and composition.

The mass flux of the component 1 is:

$$\mathbf{J}_1(\mathbf{q}) = -n_1(\mathbf{q})\hat{\mathbf{D}}_T(\mathbf{q}).\frac{\partial\delta n_1(\mathbf{q})}{\partial\mathbf{q}}$$

$$= -n_1(\mathbf{q})D_T(\mathbf{q})\frac{\partial\delta n_1(\mathbf{q})}{\partial\mathbf{q}}$$

$\delta n_1(\mathbf{q})$ is the deviation of the nonequilibrium number density of the component 1 from its equilibrium value, $n_1(\mathbf{q})$.

$$D_T(\mathbf{q}) = \frac{3\tau_d(\mathbf{q})}{2\sigma^2 \nu_1(\mathbf{q})}\sqrt{\frac{\pi}{m\beta}}$$

The zero-order approximation to the self-diffusion coefficient measured experimentally,

$$D_P(\mathbf{q}) = \nu_1(\mathbf{q})\, D_T(\mathbf{q})$$

$$= \frac{3}{2\sigma^2}\sqrt{\frac{\pi}{m\beta}}\,\tau_d(\mathbf{q})$$

$$= \frac{\frac{3}{2\sigma^2}\sqrt{\frac{\pi}{m\beta}}}{\left[\int d\hat{\mathbf{s}}\, n(\mathbf{q}-\sigma\hat{\mathbf{s}})\, g(\mathbf{q},\mathbf{q}-\sigma\hat{\mathbf{s}}) + \frac{\sqrt{2}\sigma_{fw}^2}{\sigma^2}\int d\hat{\mathbf{s}}\, n_w(\mathbf{q}-\sigma_{fw}\hat{\mathbf{s}})\, g_{fw}(\mathbf{q},\mathbf{q}-\sigma_{fw}\hat{\mathbf{s}})\right]}$$

Introducing the notations:

$$D_P^{ff}(\mathbf{q}) = \frac{3}{2\sigma^2}\sqrt{\frac{\pi}{m\beta}}\,\frac{1}{\int d\hat{\mathbf{s}}\, n(\mathbf{q}-\sigma\hat{\mathbf{s}})\, g(\mathbf{q},\mathbf{q}-\sigma\hat{\mathbf{s}})}$$

$$D_P^{fw}(\mathbf{q}) = \frac{3}{4\sigma_{fw}^2}\sqrt{\frac{2\pi}{m\beta}}\,\frac{1}{\int d\hat{\mathbf{s}}\, n_w(\mathbf{q}-\sigma_{fw}\hat{\mathbf{s}})\, g_{fw}(\mathbf{q},\mathbf{q}-\sigma_{fw}\hat{\mathbf{s}})}$$

one can rewrite the above equation in the familiar form

$$\frac{1}{D_P(\mathbf{q})} = \frac{1}{D_P^{ff}(\mathbf{q})} + \frac{1}{D_P^{fw}(\mathbf{q})}$$

Introducing dimensionless quantities:

$\mathbf{q}^* = \mathbf{q}/s_w$, $n^*(\mathbf{q}^*) = s_w^3 n(\mathbf{q}^*)$, $n_w^*(\mathbf{q}^*) = s_w^3 n_w(\mathbf{q}^*)$, and

$D_P^*(\mathbf{q}^*) = D_P(\mathbf{q}^*)/D^0$, $D_P^{ff*}(\mathbf{q}^*) = D_P^{ff}(\mathbf{q}^*)/D^0$ and $D_P^{fw*}(\mathbf{q}^*) = D_P^{fw}(\mathbf{q}^*)/D^0$

where

$D^0 = \frac{3}{2}\sqrt{\frac{p}{bm}}\, s_w$, one has:

$$D_P^{ff*}(\mathbf{q}^*) = \frac{s_w^2}{s^2 \int d\hat{\mathbf{s}}\, n^*\left(\mathbf{q}^* - \frac{s}{s_w}\hat{\mathbf{s}}\right) g\left(\mathbf{q}^*, \mathbf{q}^* - \frac{s}{s_w}\hat{\mathbf{s}}\right)},$$

$$D_P^{fw*}(\mathbf{q}^*) = \frac{s_w^2}{\sqrt{2}\, s_{fw}^2 \int d\hat{\mathbf{s}}\, n_w^*\left(\mathbf{q}^* - \frac{s_{fw}}{s_w}\hat{\mathbf{s}}\right) g_{fw}\left(\mathbf{q}^*, \mathbf{q}^* - \frac{s_{fw}}{s_w}\hat{\mathbf{s}}\right)},$$

B) PG - THERY/EMD COMPUTATIONS

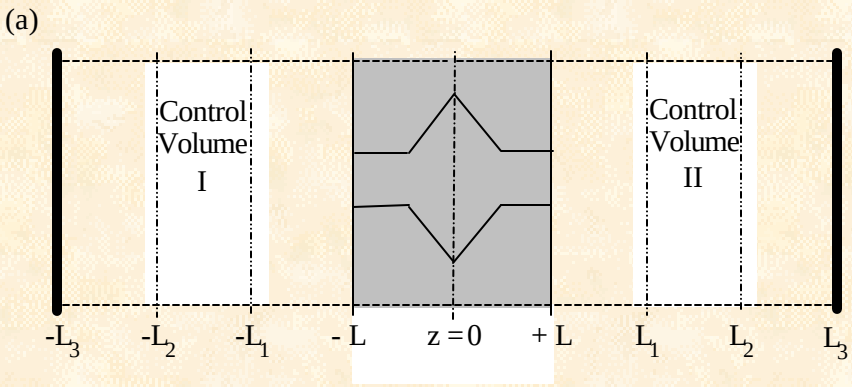

Figure 2. Model system studied in this work by the PG-theoretical and MD simulations means. (a) The fundamental cell (imaged in the x and z directions) with control volumes I and II; (b) side view of the nanopore system; (c) pore face. The axial half length, L, of the composite pore was $L_s+2.5\sqrt{2}$; the square channel: $L_s=3.5\sqrt{2}$; width: $d_s = 3\sqrt{2}$. The central unit ("octahedron"): maximum dimension $d_o = 8\sqrt{2}$. The pore system is composed of two dense face-centred cubic layers of immobile atoms. The bulk regions: $L_3 = \pm (18.5\sqrt{2} + L_s)$. Control volumes: $-L_2 < z < -L_1$; $L_1 < z < L_2$, where $L_1 = (10.5\sqrt{2} + L_s -5/3)$ and $L_2 = L_1 + 5/3$.

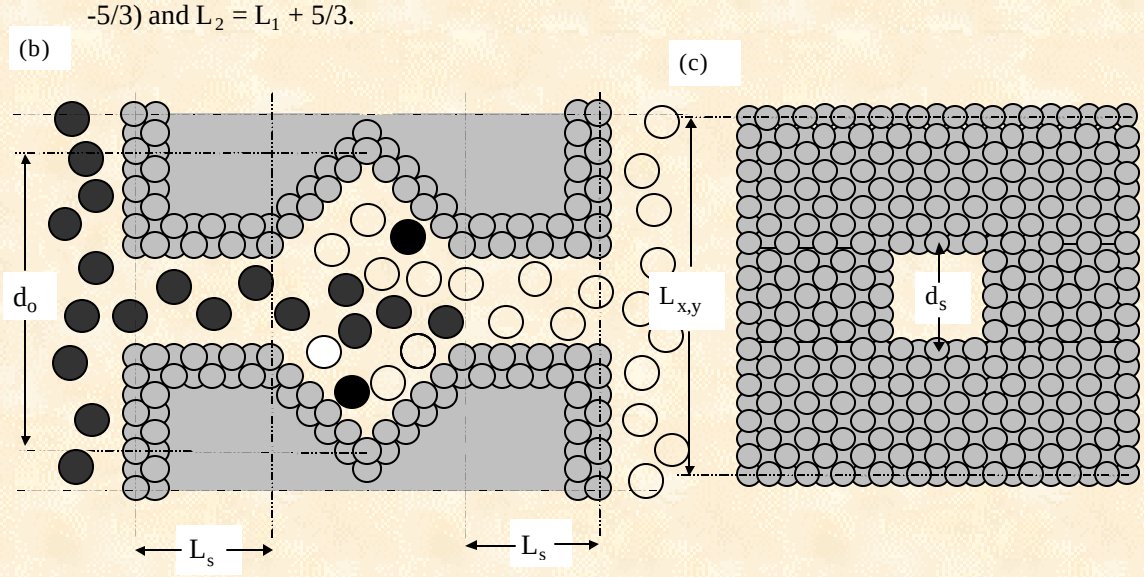

SIMULATION CONDITIONS

$$f_{ij}^{SF}(r_{ij}) = f_{ij}(r_{ij}) - f_{ij}(r_{cut}) - \left(\frac{d f_{ij}(r_{ij})}{dr_{ij}}\right)_{r_{cut}} (r_{ij} - r_{cut}); \qquad r_{ij} \le r_{cut}$$

$$= 0; \qquad r_{ij} > r_{cut}$$

with

$$f_{ij}(r_{ij}) = 4e_{ij}\left(\left(\frac{s_{ij}}{r_{ij}}\right)^{12} - \left(\frac{s_{ij}}{r_{ij}}\right)^{6}\right),$$

Table 1. Parameters of the Lennard-Jones potentials.

Component pair	σ , Å	ε/k (K)
Fluid-fluid	3.817	148.2
Wall-wall	3.000	228.4
Fluid-wall	3.409	184.0

Fluid parameters: the average number density in the "bulk" volumes, $n^* = 0.5\,s^3$, where s is the LJ-diameter of the fluid particles; the dimensionless temperature, $T^*=k_BT/e = 1.5$. The average number density of the confined nanofluid, $n_f^*=(0.4\pm0.04)\sigma^3$. **Note**: bulk fluid of similar potential parameters at this density and temperature possesses a pressure of about 220 atm; the self-diffusion coefficient for the model Lennard-Jones fluid in the bulk state has been independently determined using traditional EMD procedures to be 3.4 x 10^{-4} cm^2/s.

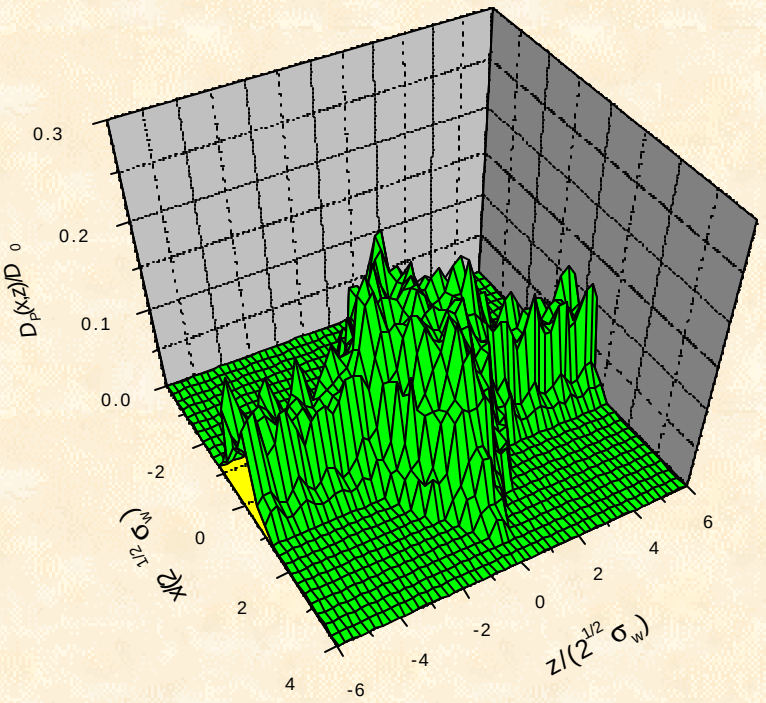

Figure 3. Zero-order approximation of the PG-theoretical self-diffusion coefficient for the entire pore system in the plane y=0.

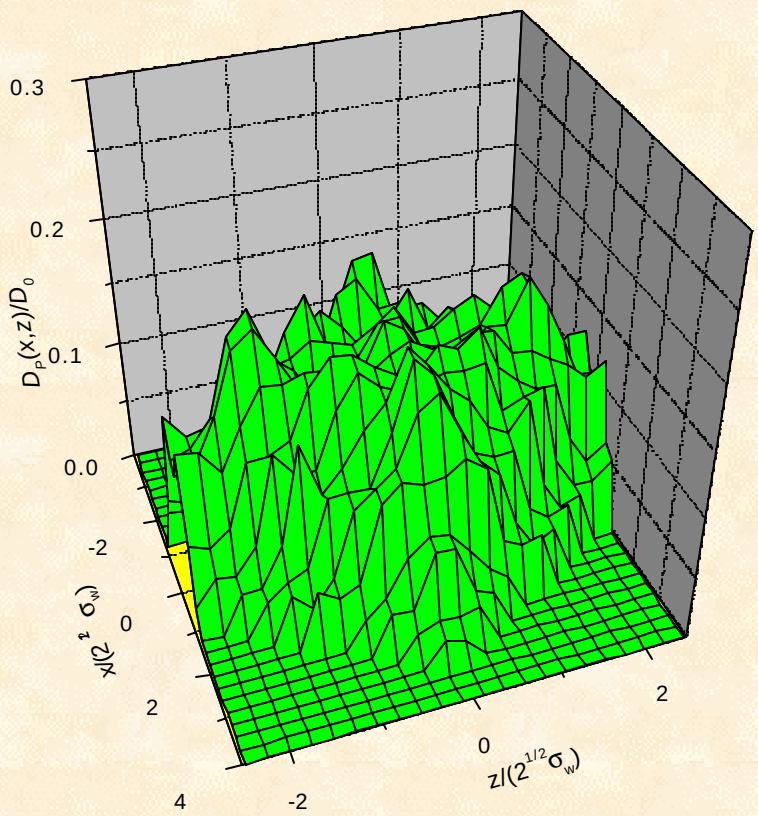

Figure 4. Zero-order approximation of the PG-theoretical self-diffusion coefficient for the central cross-section of the "octahedron" cavity at y=0

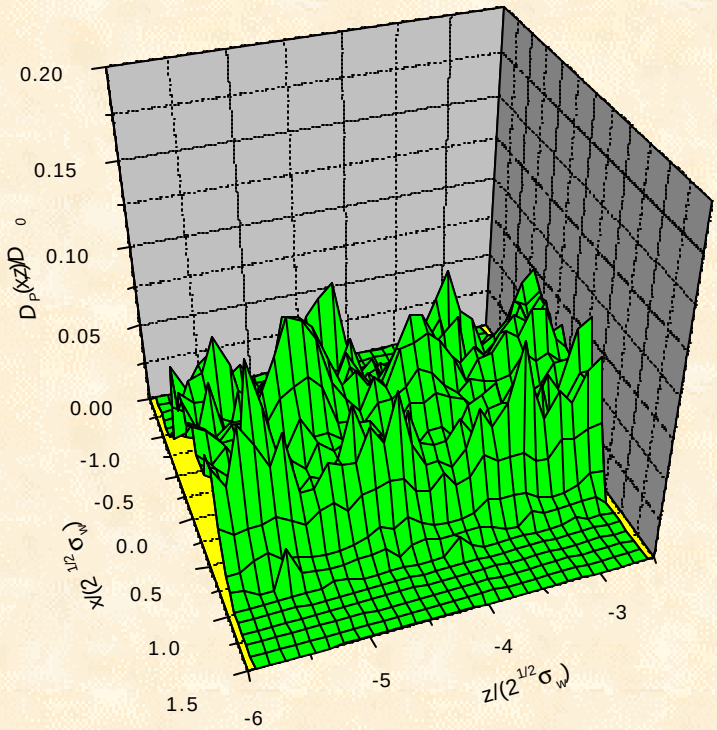

Figure 5. Zero-order approximation of the PG- theoretical self-diffusion coefficient for the square channel in the plane y=0

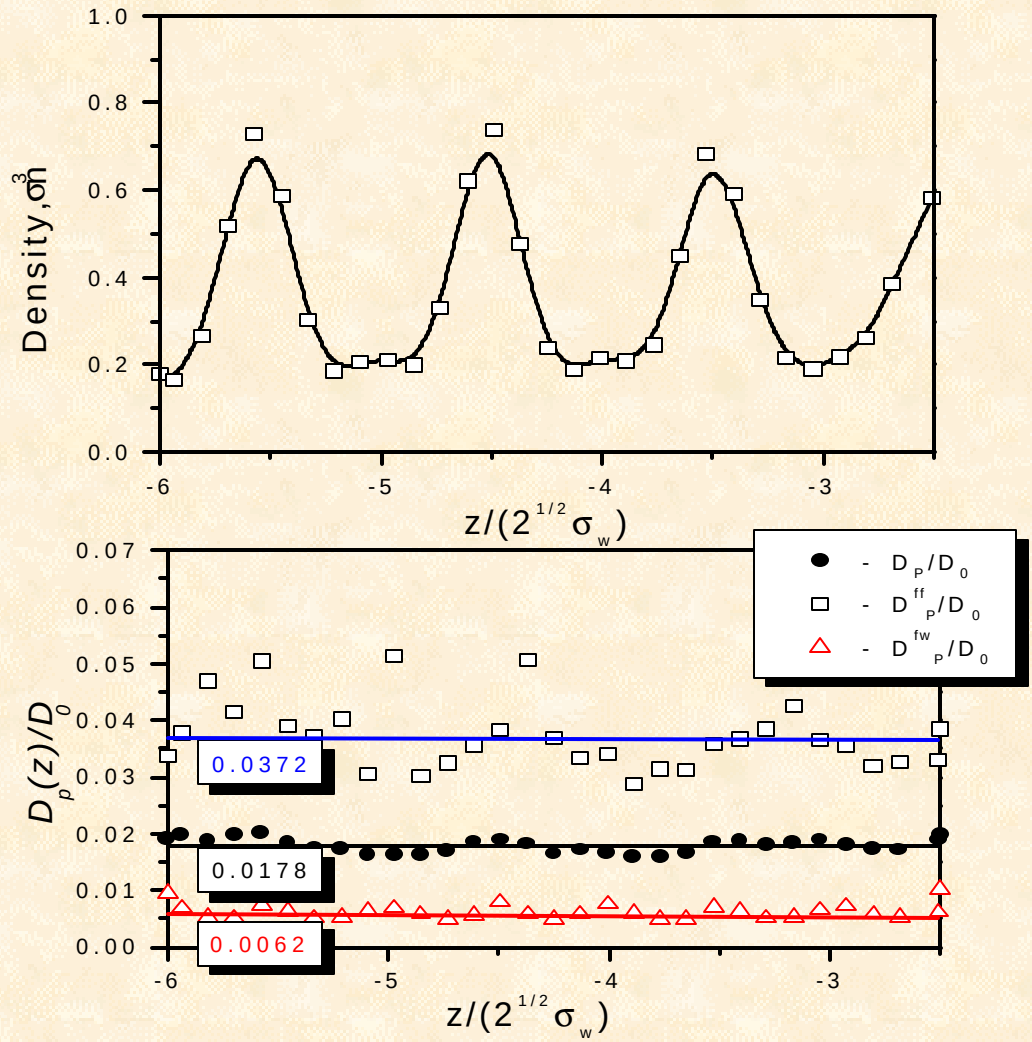

Figure 6. Top : the average nanofluid density (based on pore cross-section) for z-bins within the left square channel (open squares); the curve corresponds to a fit by B-splines.
Bottom: the fluid-fluid and fluid-wall contributions, D^{ff}_P/D^0 (open squares) and D^{fw}_P/D^0 (open triangles), respectively, to the zero-order approximation of the across-the-pore average of the PG-theoretical self-diffusion coefficient for the square channel. The horizontal lines correspond to the average values which in each case are $< D^{ff}_P/D^0 > = 0.0372$; $< D^{fw}_P/D^0 > = 0.0062$; and overall (the filled circles) $< D_P/D^0 > = 0.0178$; $D^0 = 2.715\times10^{-3}$ cm²/s.

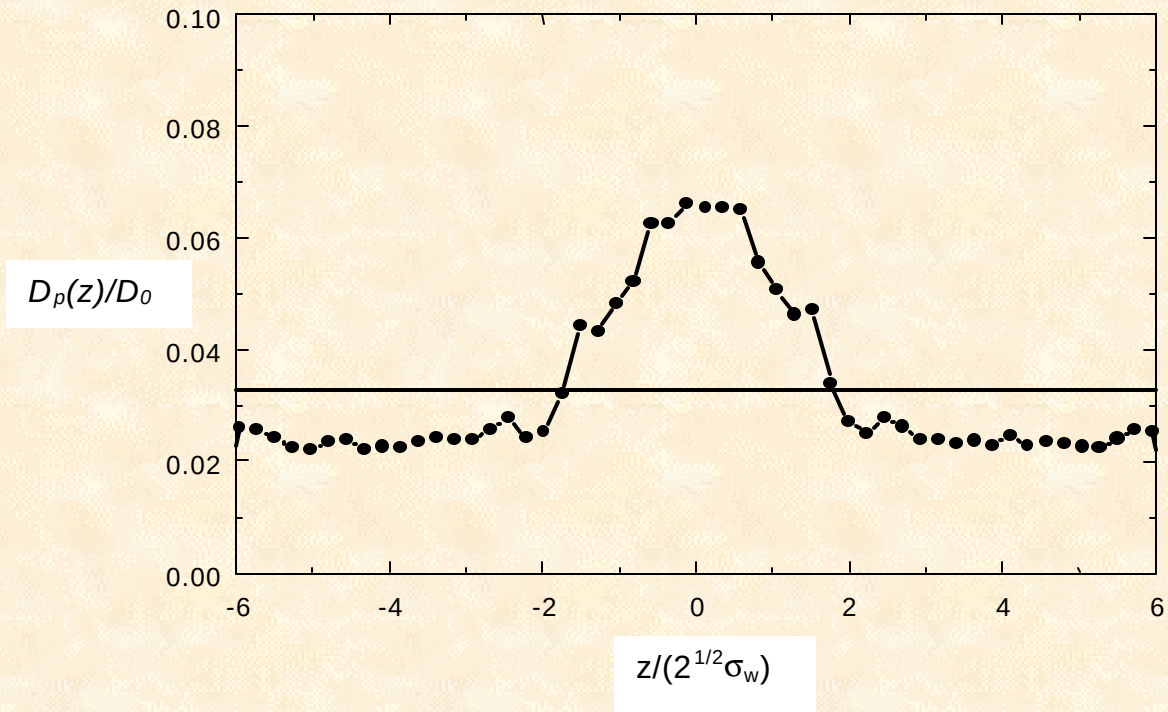

Figure 7. Zero-order approximation for the across-the-pore average of the PG-theoretical self-diffusion coefficient for the pore system. The horizontal line corresponds to the overall average value of the theoretical self-diffusion coefficient; $D^0 = 2.715\times10^{-3}$ cm^2/s.

C) NEMD SIMULATIONS AND COMPARISON OF THE RESULTS

The mass flux:

$$\bar{J}_1^z = \frac{1}{A}\int J_1^z \, dxdy$$

$$= -\left[\frac{\int D_P(\mathbf{q})\frac{\partial \, d\, n_1(\mathbf{q})}{\partial \, z}dxdy}{\int \frac{\partial \, d\, n_1(\mathbf{q})}{\partial \, z}dxdy}\right]\frac{1}{A}\int \frac{\partial \, d\, n_1(\mathbf{q})}{\partial \, z}dxdy$$

$$= -\bar{D}_P(z)\frac{\partial \, d\, \bar{n}_1(z)}{\partial \, z}$$

This expression is purely empirical and relies on considerations related to symmetries of the considered system.

Table 2. The self-diffusion coefficient of the pore nanofluid.

Pore section	Square channel	"Octahedron" section	Entire pore
Theoretical average value $D_P \cdot 10^4 \left(\frac{cm^2}{s}\right)$	0.483	1.232	0.894
NEMD value using Eqs. (15) and (16) $D_{NEMD} \cdot 10^4 \left(\frac{cm^2}{s}\right)$	0.57	0.76	-
$\frac{D_P - D_{NEMD}}{D_{NEMD}} \cdot 100\%$	-15.2	62.1	-

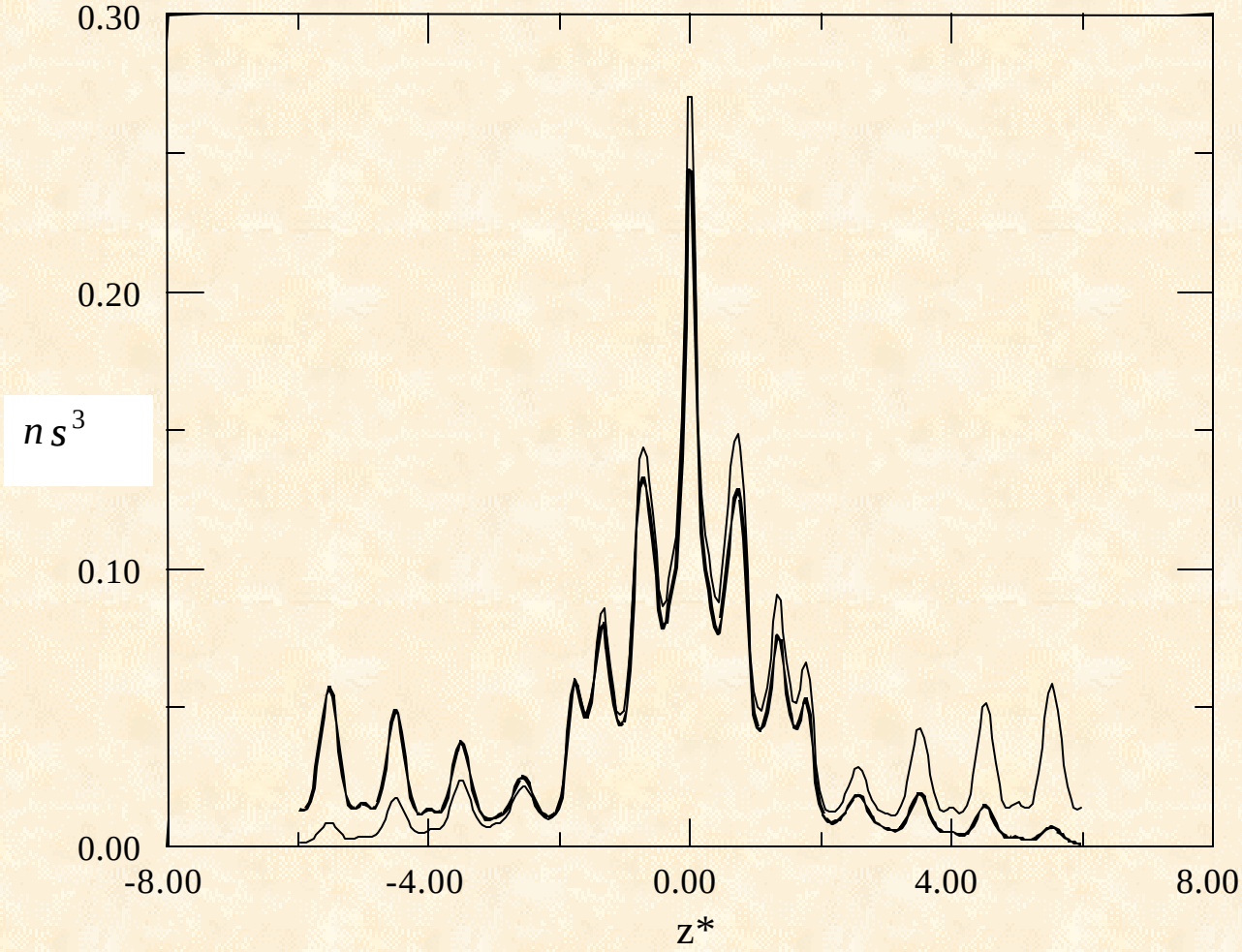

Figure 8. The non-equilibrium density profile of the counter-diffusing components expressed in the units of s^3 specific to the fluid atomic diameter; z* is in units of $\sqrt{2}s_w$.

4. CONCLUSIONS

1. The use of fundamental statistical mechanical analysis allows to investigate transport processes at nanoscale (including quantum contributions) and has a potential to suggest and verify optimal parameters of the desirable regimes of film development to meet engineering and technological requirements.

2. Rigorous statistical mechanical theoretical approaches used in conjunction with EMD and, to some extent, with NEMD techniques, have to be used to facilitate such an analysis. At present, Pozhar-Gubbins approach is the most tractable among existing rigorous statistical mechanical approaches that can be used for this purpose.

3. Due to non-local nature of the transport coefficients in nanosystems and expected large quantum contributions to them, a heuristic analysis of molecular simulation data is unlikely to be helpful in conjunction with virtual fabrication of nanoheterostructures. In general, extreme care should be exercised when attempting to interpret local transport behaviour from coarse-grained data and/or heuristic evaluations.

ACKNOWLEDGEMENTS

This work was supported by the project No. KC0203020 from the Division of Material Sciences, Office of Science, the U.S. Department of Energy, through the contract No. DE-AC05-00OR22725. The authors thank J.M.D. MacElroy for fruitful collaboration, and E. Kontar for programming support.